

Design of a high efficiency and low EMI boost converter using bi-frequency PFM control scheme

Changyuan Chang¹ · Chengèn Wu¹ · Yubo Yuan¹ · Junjie Hu¹ · Bin Bian¹

Received: 12 April 2015 / Revised: 29 May 2015 / Accepted: 18 July 2015 / Published online: 8 August 2015
© Springer Science+Business Media New York 2015

Abstract A bi-frequency PFM controlled boost DC–DC converter, combining the respective advantages of the conventional PWM and PFM, is designed and implemented in this paper to improve the electro-magnetic interference (EMI) and efficiency of the system in a wide load range. The spectral energy of proposed bi-frequency PFM controlled converter is distributed to more frequency points to decrease the discrete harmonic peak, achieving low EMI and noise level. By detecting load changes, the proposed converter operates at a corresponding frequency at light load or heavy load and switches between the two frequencies at medium load to improve full-load efficiency. A control IC for the boost converter has been fabricated in Founder Microelectronics 0.5 μm CMOS process. The layout area is $800 \times 640 \mu\text{m}^2$. Experimental results show that the full-load conversion efficiency is over 80 %, and the quiescent current is under 10 μA . Meanwhile, the converter has fine EMI characteristics.

Keywords Bi-frequency modulation · Dual-oscillator · Boost DC–DC converter · EMI · Full load efficiency

1 Introduction

In recent years, high efficiency and small EMI of DC–DC converter have become hot research directions with the continuous development of portable electronic products. Pulse width modulation (PWM) and Pulse frequency

modulation (PFM) are two popular control modes in DC–DC converters. In order to make sure that the system can operate properly at heavy load, higher frequency in the PWM controlled converter should be chosen. However, it will result in low efficiency under light load. As portable electronic products mostly work in the light load or standby mode, the PFM control scheme is more widely adopted than PWM control scheme in the DC–DC converter to reduce power consumption, effectively.

There are many kinds of PFM modes to regulate the output voltage by changing its frequency, such as forced PFM mode [1], burst mode [2], and skip mode [3]. But PFM also has some disadvantages, such as narrow frequency spectrum [4], large output ripple and large EMI [5]. As a relatively novel pulse control scheme, bi-frequency control technique, combining advantages of the frequency dithering control [6] and fixed frequency PWM control technology, appears firstly in [7] to reduce the EMI. Though this paper only illustrates the single working condition of soft-switching quasi-resonant converter, it is of considerable significance for further studies. A bi-frequency controlled buck converter has been proposed in [8] which has low-frequency and high-frequency switches, as a compromise solution to the contradiction between “high frequency” and “efficiency”. This method is applicable to medium and high power occasions, but its circuit is very complex. A bi-frequency controlled DC–DC converter has been presented in [9], which only gives system model and simulation verification of the boost converter based on the control technique. A new bi-frequency constant real-time control technology has been proposed in [10], but the mainly focus on theoretical study and system analysis, without specific actual circuit design, is its drawback.

Based on the above analysis, this paper proposes a boost converter, adopting bi-frequency control scheme, to obtain

✉ Changyuan Chang
ccycc@seu.edu.cn

¹ School of Integrated Circuit, Southeast University, Nanjing 210096, People’s Republic of China

better EMI performance and higher conversion efficiency. The operation principle of proposed Bi-frequency PFM controller for DC–DC boost converter is analyzed in Sect. 2, and circuit design consideration is given in Sect. 3. Section 4 shows the layout and test results, based on Founder Microelectronics 0.5 μm CMOS process.

2 Operation principle of a bi-frequency PFM controller

The system diagram of proposed boost converter is shown in Fig. 1. The voltage comparator [11, 12] generates different control signals V_{comp} to select different frequencies, depending on the load conditions. By detecting V_{comp} , the bi-frequency oscillator outputs a corresponding switching signal CLK to the driving circuit, adjusting the output voltage V_o . EN is the enable signal determining whether the bi-frequency PFM controller works or not. The hysteresis comparator disables the CLK signal at extreme light load, when the low frequency may not be low enough to stabilize the output voltage V_o .

Figure 2 shows the typical operation waveform of proposed bi-frequency control scheme. Where f_H is the high frequency of bi-frequency oscillator, T_H is the corresponding period; f_L is the low frequency of bi-frequency oscillator, T_L is the corresponding period; T_{on} is the turn-on time of the power switch. The basic working principle can be illustrated as follows: the bi-frequency PFM controller outputs high frequency signal to the driving circuit when feedback voltage V_{fb} (see in Fig. 1) is lower than the reference voltage V_{ref} ; otherwise outputting low frequency signal.

The efficiency of the PWM converter is:

$$\eta_{pwm} = \frac{\frac{V_o^2}{R_L}}{\frac{V_o^2}{R_L} + W_{LOSS}} = \frac{V_o^2}{V_o^2 + (f_e \times W_{SW} + W_{CON}) \times R_L} \quad (1)$$

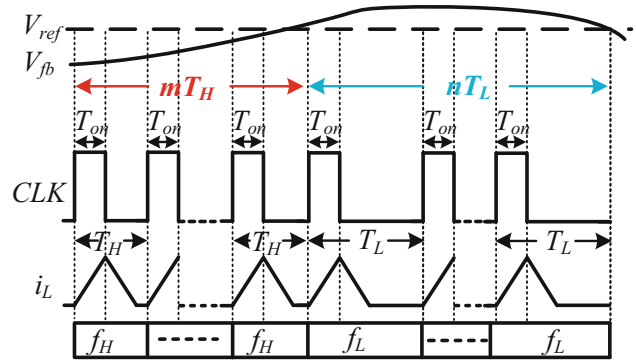


Fig. 2 Operation waveform of proposed bi-frequency control scheme

The efficiency of the bi-frequency PFM converter is:

$$\eta_{bif} = \frac{\frac{V_o^2}{R_L}}{\frac{V_o^2}{R_L} + W_{LOSS}} = \frac{\frac{V_{in} T_{on} V_o (1 - D_{on})}{2L}}{\frac{V_{in} T_{on} V_o (1 - D_{on})}{2L} + (f_e \times W_{SW} + W_{CON})} \quad (2)$$

where W_{SW} is equivalent to the switching loss, W_{CON} is the conduction loss of power tube, W_{LOSS} is the sum of switching loss and conduction loss, D_{on} is the equivalent duty ratio, f_e is the equivalent frequency.

It can be seen from (1) and (2) that the efficiency of the PWM control scheme will be significantly reduced with the increasing of load resistance R_L , because its frequency is constant under light load operation. However, the efficiency of the bi-frequency PFM control scheme is only determined by the equivalent frequency f_e (f_e is relatively low), which is independent from R_L . Therefore, the bi-frequency PFM scheme can effectively improve the efficiency under light load.

In addition, the bi-frequency PFM control signal CLK consists of m high-frequency pulses of f_H and n low-frequency pulses of f_L according to the load condition.

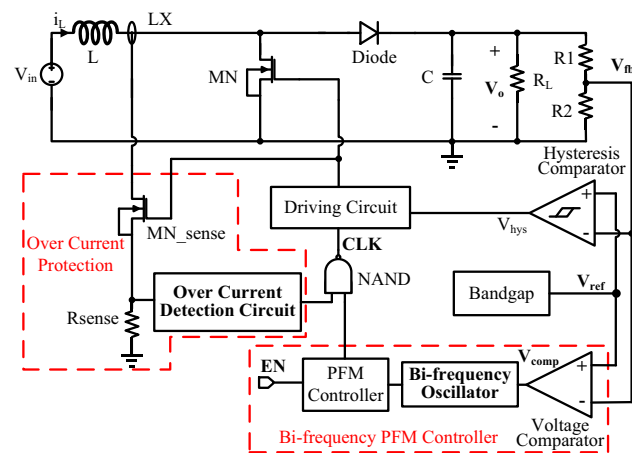


Fig. 1 System diagram of proposed boost converter

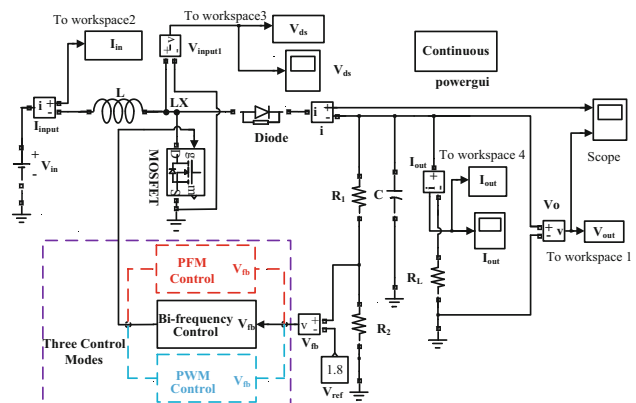


Fig. 3 System model of the boost converter using three control schemes, respectively

Therefore, the Fourier transform of the proposed bi-frequency PFM control signal is:

$$F_{BF}(f) = 2\pi f_M \sum_{n=-\infty}^{+\infty} |F_{f_1(t)}(nf_M)| \delta(f - nf_M) \tag{3}$$

$$F_{f_1(t)}(f) = T_{on} Sa(\pi f T_{on}) \left(\frac{1 - e^{-j2\pi f m T_H}}{1 - e^{-j2\pi f T_H}} + e^{-j2\pi f m T_H} \frac{1 - e^{-j2\pi f n T_L}}{1 - e^{-j2\pi f T_L}} \right) \tag{4}$$

where $f_M = 1/(mT_H + nT_L)$, $|\cdot|$ is modular arithmetic.

While the Fourier transform of the PWM and PFM control signals are:

$$F_{PWM}(f) = 2\pi D \sum_{n=-\infty}^{+\infty} \left| \frac{\sin(n\pi D)}{n\pi D} \right| \delta(f - nf_s) \tag{5}$$

$$F_{PFM}(f) = 2\pi f_e \sum_{n=-\infty}^{+\infty} \left| Sa\left(\frac{n\pi f_e}{2}\right) \right| \delta(f - nf_e) \tag{6}$$

where D is the duty cycle, f_s is the switching frequency.

Compared with traditional PFM mode and PWM mode, the spectrum of the bi-frequency PFM control signal is no longer isolated and scattered. Besides, it has a large number of side frequencies and the spectrum energy is distributed to more frequency points to decrease the discrete harmonic peak, achieving low EMI and noise level. Consequently, the DC–DC converter with bi-frequency PFM mode is easier to meet the EMI standards.

3 Circuit design consideration

The proposed Bi-frequency PFM controller needs to generate two frequency signals f_L and f_H , corresponding to two duty cycle D_L and D_H , to meet different input voltages and load changes. The relationship between the input voltage V_{in} and output voltage V_o of the boost circuit is given by [13]:

$$V_{in} \frac{1}{1 - D_{on}} = V_o \tag{7}$$

If the circuit can work properly at 2 V, and the output voltage V_o can achieve 5 V, then the minimum D_{on} is 60 %. Another case, if the input voltage is 4 V and output voltage is 5 V, the corresponding D_{on} will be about 20 %. In actual bi-frequency PFM control scheme, the paper sets a low frequency f_L and a high frequency f_H . T_{on} is a fixed value, i.e. $f_L T_{on} = D_L = 20\%$, $f_H T_{on} = D_H = 60\%$. Thus

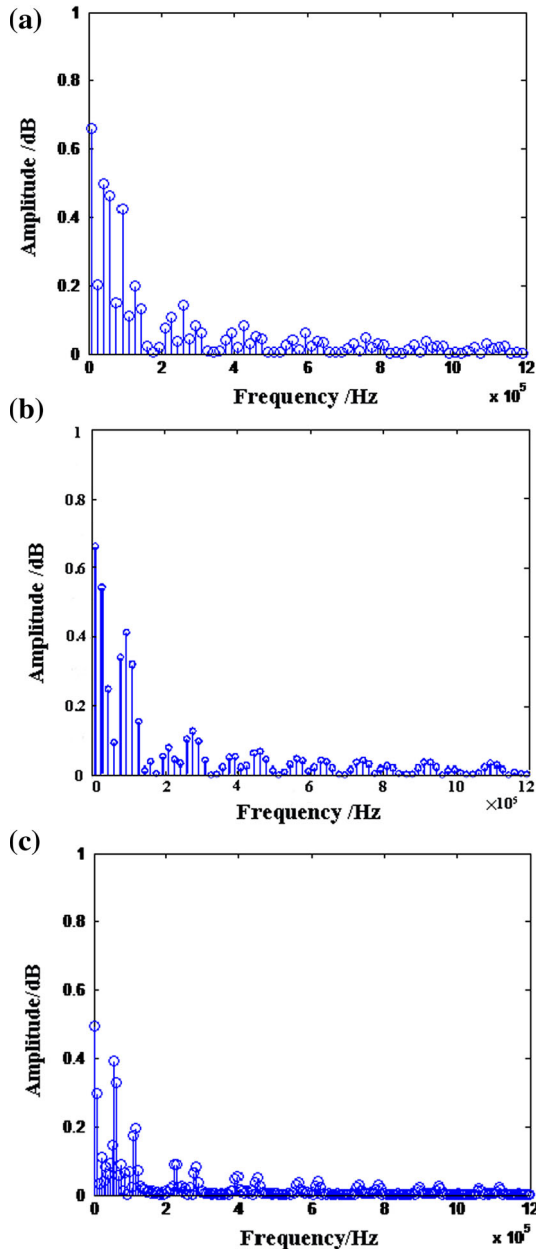


Fig. 4 Frequency spectrum of LX signal under different control schemes. **a** PWM control scheme. **b** PFM control scheme. **c** BF-PFM control scheme

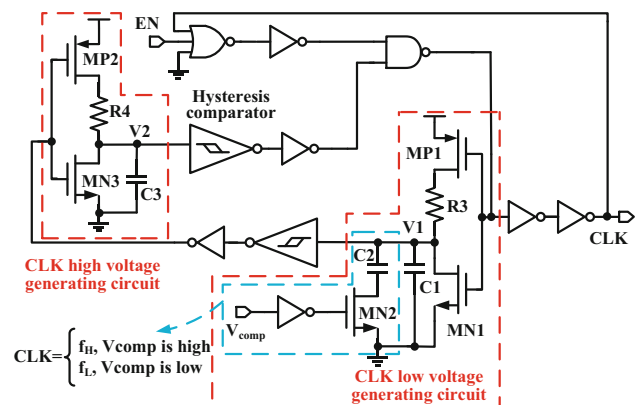


Fig. 5 Circuit of bi-frequency oscillator

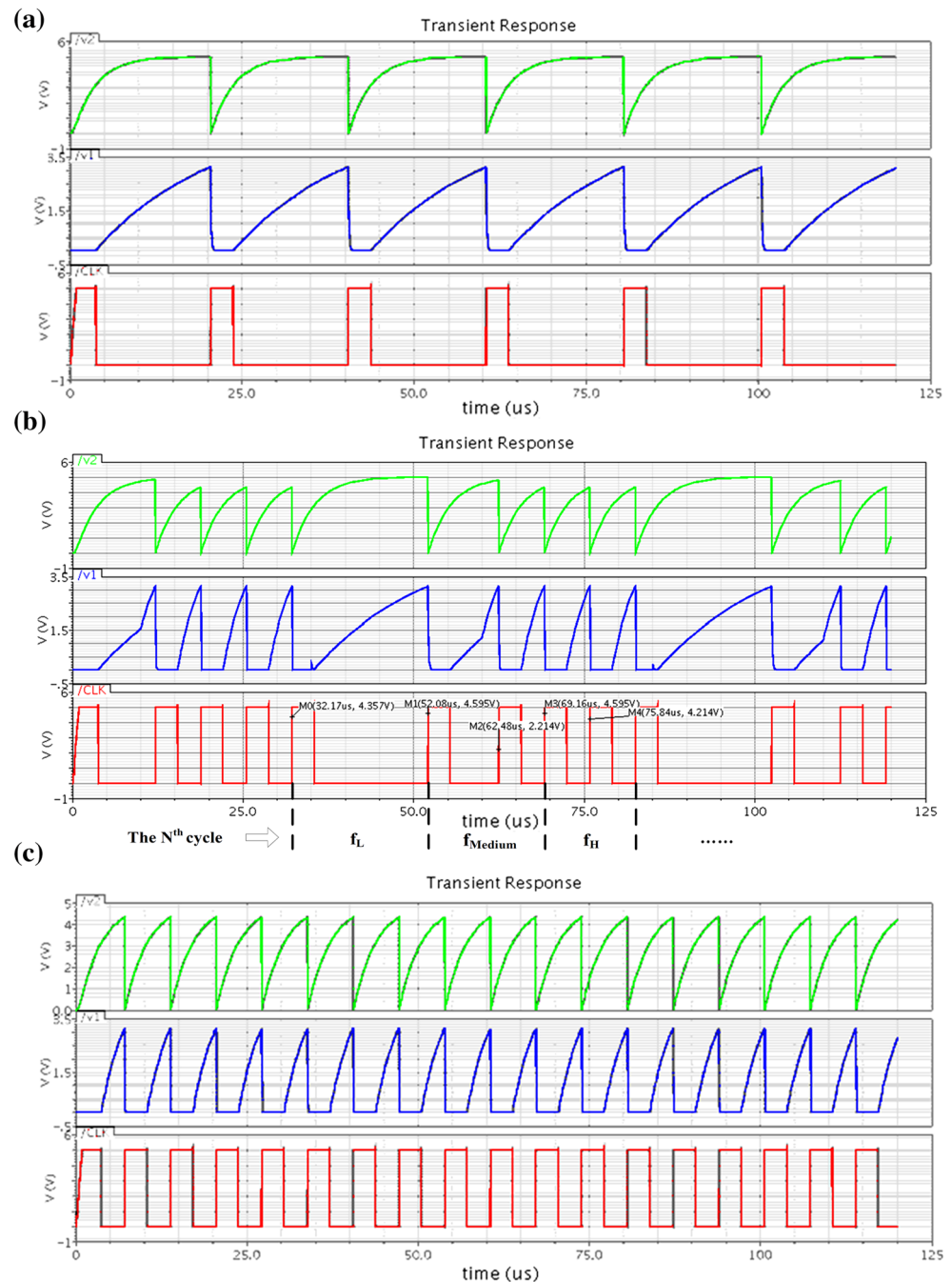
$f_L:f_H = 1:3$. Considering the ripple and efficiency factors, the two frequencies of the oscillator are set as $f_L = 50$ kHz, $f_H = 150$ kHz.

3.1 System design consideration

Based on the above analysis, the system model of the boost converter, respectively using three control modes, is built in Matlab/Simulink as shown in Fig. 3.

The frequency spectrums of voltage signal LX of boost converter, using different modulation methods, are compared in Fig. 4. The comparison of Fig. 4(a), (b), (c) shows that frequency spectrum of LX of the boost converter with bi-frequency PFM controller has the most numerous harmonic components, which means that its spectral energy can be dispersed into more frequency points than that of PWM and PFM, so that its discrete harmonic peaks are lower. Consequently, the boost converter has less EMI

Fig. 6 CLK signal output waveforms under different load currents. **a** Light load ($I_{load} = 50$ mA). **b** Medium load ($I_{load} = 120$ mA). **c** Heavy load ($I_{load} = 170$ mA)



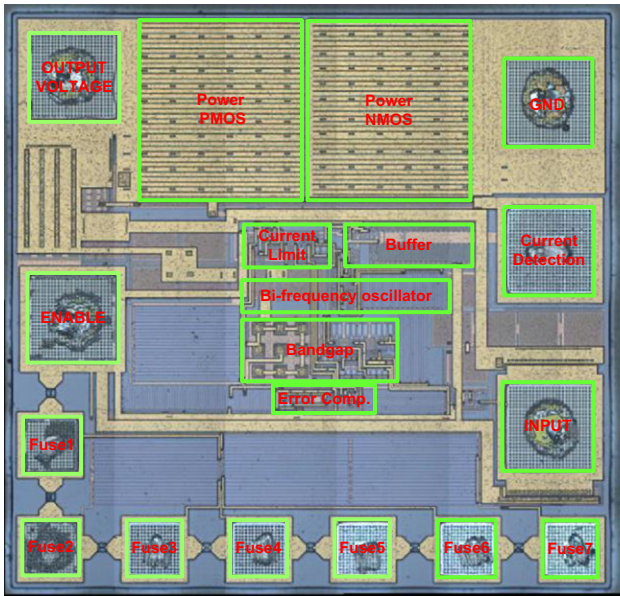


Fig. 7 Chip layout micro photograph

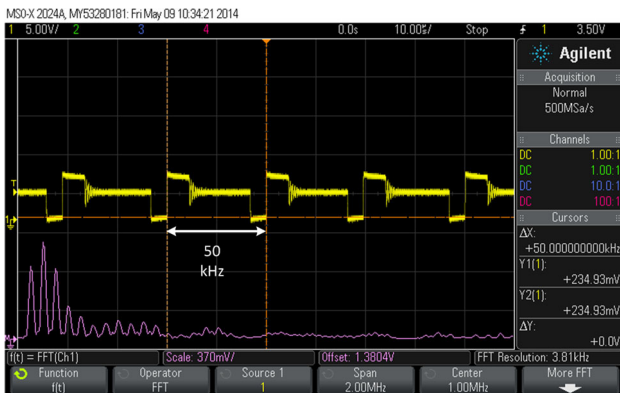


Fig. 8 The LX and V_o waveforms under light load (50 mA)

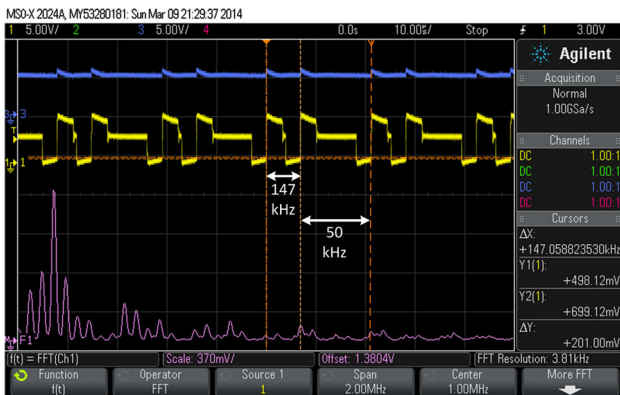


Fig. 9 The LX and V_o waveforms under medium load (120 mA)

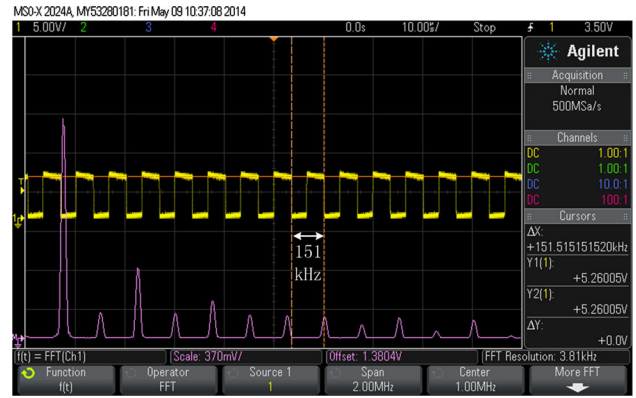


Fig. 10 The LX and V_o waveforms under heavy load (170 mA)

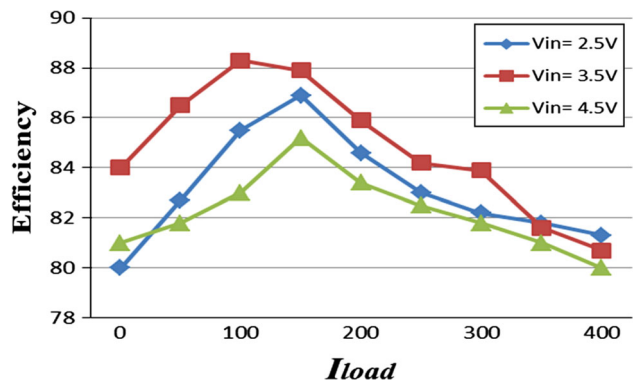


Fig. 11 Relationship of load current versus conversion efficiency

Table 1 Main performance of the proposed converter

Parameter	Text
Input voltage range	2–5 V
Operating frequency	f_L : 50 kHz; f_H : 150 kHz
Maximum conversion efficiency	88.3 %
Load regulation ($I_{load} = 5\text{--}300\text{ Ma}$)	2.23 (%/mA)
Typical output voltage	5 V
Overall conversion efficiency	>80 %
Line regulation ($V_{in} = 2\text{--}5\text{ V}$)	2.85 (%/V)

noise and can be easier to meet corresponding EMI standards.

3.2 Key circuit design

As shown in Fig. 5, the proposed bi-frequency oscillator is mainly composed by CLK low voltage generating circuit, CLK high voltage generating circuit, two hysteresis comparators, six inverters, a Nor gate and a Nand gate. V_{comp} is the output signal of voltage comparator in Fig. 1, which

is low when V_{fb} is higher than V_{ref} and high on the opposite. When V_{comp} is high, capacitor $C2$ does not work, the output signal of CLK will be f_H , and CLK will be f_L when V_{comp} is low. $V1$, $V2$ is the output voltage of low voltage generating circuit and CLK high voltage generating circuit, respectively. In the bi-frequency oscillator, CLK high voltage generating circuit is designed to implement the T_{on} part of the CLK signal, while CLK low voltage generating circuit, based on the load condition represented in V_{comp} , generates the low voltage part of CLK to obtain two specific frequency f_L and f_H by changing the charging capacitor between $C1$ and $C1 + C2$, respectively.

The general operation principle is as follows: when the voltage signal CLK is low at the beginning, capacitors $C1$, $C3$ or $C1$, $C2$, $C3$ are charged, the corresponding voltage $V1$ and $V2$ increase. The increasing speed of $V2$ is faster than that of $V1$, but CLK does not step to high voltage until $V1$ passes the reverse voltage of the hysteresis comparator. Meanwhile, both the voltages of CLK and $V1$ are high, capacitors discharge quickly, $V1$ and $V2$ decrease to zero. And then, $C3$ is charged, $V2$ starts to increase. When $V2$ passes the reverse voltage of the hysteresis comparator, CLK turns to be low voltage. And that cycle repeats. Therefore, the bi-frequency oscillator outputs low frequency signal f_L at light load, high frequency signal f_H at heavy load, and switches between f_L and f_H to regulate the output voltage V_o at medium load. As Eqs. (3) and (4) illustrate: CLK consists of m cycles of f_H , and n cycles of f_L , the lighter load is, the smaller m and bigger n are, correspondingly, which is consistent with the simulation results in Fig. 6.

Furthermore, input voltage of the circuit is 2.5 V, while output voltage under different load conditions are maintained at about 5 V, so the system can achieve step-up and regulator function.

4 Layout design and testing

The proposed controller is fabricated in Founder Microelectronics 0.5 μm CMOS process and the area is $800 \mu\text{m} \times 640 \mu\text{m}$, as is shown in Fig. 7. Test conditions of the bi-frequency controlled converter are as follows: the input voltage $V_{in} = 2.5 \text{ V}$, load current I_{load} varies from 0 to 300 mA and the selected central frequency is 1 MHz. Meanwhile, it sweeps from 0 to 2 MHz.

When load current is 50 mA (light load), the LX and V_o waveforms are shown as Fig. 8: the LX square waves are

all low frequency signals. A diode connects the output and LX, so there is a certain voltage drop between them. It can be seen that, considering the LX output waveform under medium load (120 mA) in Fig. 9, some high frequency signals appear in the original low frequency signals when increasing the load current. When load current increases to 170 mA (heavy load), all the LX output signals become high frequency, shown in Fig. 10.

The experimental results show that the controller can generate the control signal which switches between two fixed operating frequencies according to load changes: mainly in low frequency under light load, mainly in high frequency under heavy load, and two frequencies coexist in medium load. Therefore, the design of circuit is proved to be valid. In addition, according to the frequency spectrums of voltage signal LX showed from Figs. 8, 9, 10, the proposed bi-frequency control scheme is verified to have low EMI.

Figure 11 shows the relationship between the load current and the conversion efficiency, which refers to the ratio of output power and input power. According to Fig. 11, the conversion efficiency is more than 85 % when the load current is 120 mA. Meanwhile, Table 1 also shows that the test results basically meet the requirements of design specification.

5 Conclusion

In this paper, a bi-frequency PFM controller for boost DC–DC converter is designed and implemented. The detailed operation principle and design process are presented in this paper. The controller is fabricated in Founder Microelectronics 0.5 μm CMOS process. The experimental results show that the maximum conversion efficiency is up to 88 %, and the quiescent current is under 10 μA . Meanwhile, the spectrum energy is distributed to more frequency points. Therefore, the converter has fine EMI characteristics. So the performance of the prototype can meet the design requirements.

This control method only needs two frequencies, which means that the spectrum peak is more regular, and will be easier for the follow-up filter design to reduce EMI. In essence, the design takes full advantage of the conventional PWM and PFM. However, how to tradeoff efficiency, EMI performance and optimization of the circuit's design, still needs further study.

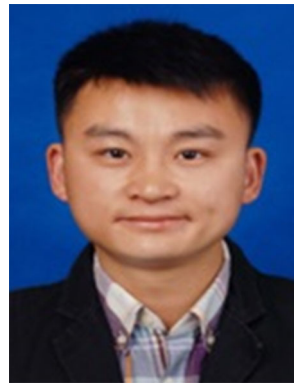
Acknowledgments This work was supported by the National Nature Science Foundation of China (61376029), the Fundamental Research Funds for the Central Universities, College Graduate Research and Innovation Program of Jiangsu Province, China (SJLX_0064).

References

1. Qahouq, J., Abdel-Rahman, O., Huang, L., & Batarseh, I. (2007). On load adaptive control of voltage regulators for power managed loads: Control schemes to improve converter efficiency and performance. *IEEE Transactions on Power Electronics*, 22(5), 1806–1819.
2. Feng, L., & Ma, D. S. (2009). An integrated switching DC-DC converter with dual-mode pulse-train/PWM control. *IEEE Transactions on Circuits and Systems II Express Briefs*, 56(2), 152–156.
3. Khaligh, A., Rahimi, A. M., & Emadi, A. (2008). Modified pulse-adjustment technique to control DC/DC converters driving variable constant-power loads. *IEEE Transactions on Industrial Electronics*, 55(3), 1133–1146.
4. Dwelley, D. M. (2001). Voltage mode feedback burst mode circuit. US Patent 6307356, Oct 2001.
5. Huang, H. W., Chen, K. H., & Kuo, S.-Y. (2007). Dithering skip modulation, width and dead time controllers in highly efficient DC-DC converters for system-on-chip applications. *IEEE Journal of Solid State Circuits*, 42(11), 2451–2465.
6. Fardoun, Abbas A., & Ismail, Esam H. (2009). Reduction of EMI in AC drives through dithering within limited switching frequency range. *IEEE Transactions on Power Electronics*, 24(3), 804–811.
7. Sun, X., Zhang, Y., Gegner, J., et al. (1993). Bi-frequency control for DC-to-DC converters. In *Proceedings of the international conference on industrial electronics, control, and instrumentation*, Vol. 2, (pp. 848–851)
8. Luo, Q. M., Zhou, L. W., Lu, W. G., et al. (2008). Performance analysis and design of double frequency buck converter. *Transactions of China Elerotechnical Society*, 23(5), 56–61.
9. Shi, G., Tang, S. L., & Luo, P. (2006). Design of a discrete pulse frequency modulation. *Microelectronics*, 36(3), 304–306.
10. Wang, J.P., Xu, J.P., Zhang, F., et al. (2010) A novel constant on-time bi-frequency control technique for switching DC-DC converters. In *proceedings of the 5th IEEE conference on industrial electronics and applications* (pp. 1094–1097)
11. Lu, J., & Holleman, J. (2013). A low-power high-precision comparator with time-domain bulk-tuned offset cancellation. *IEEE Transactions on Circuits and Systems I*, 60(5), 1158–1167.
12. Lu, J., & Holleman, J. (2012). A low-power dynamic comparator with time-domain bulk-driven offset cancellation. In *proceedings of IEEE international symposium on circuits and systems (ISCAS)* (pp. 2493–2496).
13. Santolaria, A. (2009). Effects of switching frequency modulation on the power converter's output voltage. *IEEE Transactions on Industrial Electronics*, 56(7), 2729–2737.



Changyuan Chang received his M.S. and Ph.D. degrees in Electronic Engineering from Southeast University, Nanjing, China in 1990 and 2000, respectively. He is currently an Associate Professor in the School of Integrated Circuit in Southeast University. His main research interests are in the field of Analog-controlled and digitally-controlled ICs design for power-management.



Chengèn Wu received the B.S. degree from Shanghai University of Electric Power, Shanghai, China in 2013. Now he is pursuing the M.S. degree in IC engineering at Southeast University, Nanjing, China. His research interests include non-linear modeling and design of power converters.



Yubo Yuan received the B.S. degree from Chang'an University, Xi'an, China in 2013. Now he is pursuing the M.S. degree in IC engineering at Southeast University, Nanjing, China. His research interests include control algorithm and design of power converters.



Junjie Hu was born in Hubei, China, in 1989. He received the B.S. degree from Hubei University, Wuhan, China, in 2013. He is presently pursuing the M.S. degree in microelectronics at Southeast University, Nanjing, China. He is engaged in the research on analog integrated circuits, power electronics and high-efficiency AC–DC converters.



Bin Bian received the B.S. degree in Electrical Engineering from Anhui University of Technology in 2005. From 2005 to 2009, he has mainly designed special power supply used for optical instruments in Shibuya Optical company, Japanese high-tech enterprise. Presently he is an engineer of power supply chip design and a product application technology leader in Chiplink Semiconductor company.